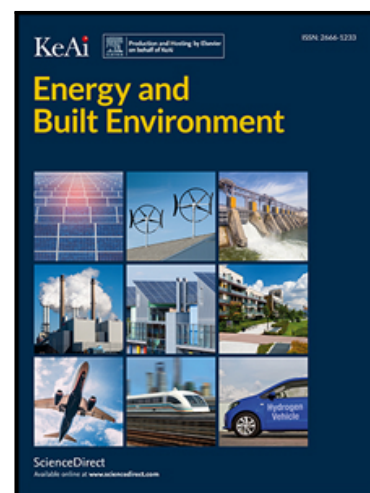


Investigation of low grade Thermal Energy Storage systems with Phase Changing Materials

Law Torres Sevilla , Jovana Radulovic

PII: S2666-1233(20)30058-1
DOI: <https://doi.org/10.1016/j.enbenv.2020.05.006>
Reference: ENBENV 49



To appear in: *Energy and Built Environment*

Received date: 5 November 2019
Revised date: 26 May 2020
Accepted date: 27 May 2020

Please cite this article as: Law Torres Sevilla , Jovana Radulovic , Investigation of low grade Thermal Energy Storage systems with Phase Changing Materials, *Energy and Built Environment* (2020), doi: <https://doi.org/10.1016/j.enbenv.2020.05.006>

This is a PDF file of an article that has undergone enhancements after acceptance, such as the addition of a cover page and metadata, and formatting for readability, but it is not yet the definitive version of record. This version will undergo additional copyediting, typesetting and review before it is published in its final form, but we are providing this version to give early visibility of the article. Please note that, during the production process, errors may be discovered which could affect the content, and all legal disclaimers that apply to the journal pertain.

© 2020 Southwest Jiaotong University. Published by Elsevier B.V.
This is an open access article under the CC BY-NC-ND license.
(<http://creativecommons.org/licenses/by-nc-nd/4.0/>)

Investigation of low grade Thermal Energy Storage systems with Phase Changing Materials

Law Torres Sevilla^a, Jovana Radulovic^a

^aSchool of Mechanical and Design Engineering, Anglesea Building, Anglesea Road, Portsmouth, United Kingdom, PO1 3DJ

law.torressevilla@port.ac.uk

Highlights

- **Paraffin wax is a good storage medium due to fast charging and good latent heat absorption.**
- **The two designs follow the same heating dynamics independently of the final temperatures reached.**
- **An addition of a second inlet yields higher final temperatures and improves the HTF distribution.**
- **This allows a better heat transfer rate, yet the temperature increase is minimal and negligible.**
- **Higher or lower velocities at the inlet(s) can benefit the system depending on the design type.**

Abstract

The use of phase changing materials (PCMs) for energy storage has been in the focus of scientific research for a while, primarily focusing on building cooling/heating applications due to favourable melting temperature ranges. In this paper we simulated the suitability of encapsulated Paraffin Wax on a small scale in a low temperature thermal energy storage system using COMSOL Multiphysics. Heat absorption and heating dynamics were analysed for different inlet designs and velocities, and the thermal gradient was evaluated across the tank geometry in a number of charging scenarios. Results show that paraffin wax proves to be a good storage medium based on its fast charging and good latent heat absorption. The study found that although an addition of a second inlet to the system yields higher final temperatures and improves the heat transfer rate, it does so minimally and therefore is not notably beneficial. Both designs follow the same heating dynamics independently on the final temperatures. Lastly, higher or lower velocities benefit the system based on the design.

1. Introduction

Energy storage is an essential component of any renewable energy system due to the intermittent character of these technologies. In times of high demand, where the sun is not shining and the wind is not blowing, the existence of a backup energy supply with easy and fast access is necessary. Heating and cooling demands account for almost half of the final energy consumption globally and since majority is based on the use of fossil fuels, it contributes to 40% of global carbon emissions [1].

Thermal Energy Storage (TES) system can be generally split into low grade and high grade. High grade energy storage allows for efficient transformation and utilisation of energy, typically employed in power systems or electricity generation. There is a lot of unexplored potential in storing heat combined with renewables, thus, low grade TES are presented as a potential solution. The aim of this study is to evaluate paraffin's suitability as a phase changing material (PCM) for two 2D tank designs using numerical methods in the software COMSOL Multiphysics.

The majority of research focuses on sensible heat and latent heat, or the combination of the two. Sensible heat is denoted by the system being added or subtracted heat without the presence of a phase change. The materials store the heat energy in their specific heat capacity per degree changed, in this case per degree increased [2]. It can be expressed as the following:

$$Q = m * C_p * \Delta T \quad (1)$$

Where Q is the total energy [kJ], m is mass [kg], C_p is specific heat capacity [kJ/kgK] and ΔT is the change in temperature [K].

Sensible heat stored is therefore proportional to density, volume, specific heat and change in temperature. Storage medium can be further categorised into liquid (water, mineral oils, molten salts, etc.) or solid (rocks, concrete, sand, etc.). Liquid mediums favour buoyancy and help create a thermal gradient, but cause leaking and vapour pressure issues. Solid ones do not have these issues and are low cost, yet have lower heat transfer efficiency [3]. Sensible systems generally offer advantages such as high thermal conductivity and low cost, making them ideal for domestic usage [4].

In terms of their operating temperatures, they depend mainly on the application of the TES and the available space. Refrigeration cycles and cooling systems range from roughly -20°C to 10°C . Common temperature ranges for medium temperatures lie between 20°C and 90°C and are typically implemented in small scale or domestic systems. Operating temperatures usually do not surpass 100°C [5,6]. These require different materials to those employed in the high temperature systems [7]. For example, thermal energy storage paired with concentrated solar development utilises molten salts with operating temperatures ranging from approximately 300 to 500°C [8]. Although molten salts are commonly used working fluids in sensible heat systems, they do they can also be used as storage materials when melted. Phase change, however, is commonly associated with latent heat systems.

Latent heat systems focus on heat absorption at the phase change of the material, where they absorb energy as their latent heat of fusion. Advantages of latent heat systems include the high energy density and narrower operational temperature range [9]. They usually combine well with low temperature applications as these require less volume for a higher output and low-grade systems tend to have more limited space [10]. For charging, which is the focus of this study, the medium state changes from liquid-gas (evaporation), solid-liquid (melting) and solid-solid [3]. For solid-solid, the

internal molecular arrangement of the solid turns from a crystalline structure to an amorphous after it reaches phase transition temperature [11].

Although liquid-gas systems have higher latent heat phase transition, they also carry large changes in volume and pressure, which adds to the cost and complexity of the system. Solid-liquid have previously proved to be the economically attractive solution and they experience small changes in volume of 10% or less. Solid-solid is becoming more popular, its interest is increasing, yet its opportunities and applications are still being discussed, which limits the amount of experimental data available [11]. The general equation for such systems is as follows:

$$Q = m[Cp1 * \Delta T + L + Cp2 * \Delta T] \quad (2)$$

Where Q is the total energy [kJ], m is mass [kg], Cp1 is specific heat capacity of the first phase [kJ/kgK], L is the latent heat energy [kJ/kg], Cp2 is specific heat capacity of the second phase [kJ/kgK] and ΔT is the change in temperature [K].

From a materials perspective, latent heat systems include organic ones (paraffins or fatty acids), inorganic (salt hydrates, low melting metals) and eutectics [12]. Fatty acids and paraffins are used in low grade systems and there is significant research done about their favourable properties as TES materials. Paraffins are suited due to their flexibility in extending their polymer chains for different melting temperatures, because they are safe, non-reactive and they have little to no supercooling [13]. Fatty acids tend to have higher latent heat of fusion, good chemical stability, and are sustainable as they are derived from vegetable and animal oils [14]. Nevertheless, they are flammable and roughly three times more expensive than paraffin [15].

Sharma et al. [16] comment on the suitability of capric acid, lauric acid, myristic acid, palmitic acid and stearic acid as PCMs for a 2D theoretical model using a shell and tube heat exchanger. They state fatty acids have favourable properties such as melting congruence, good chemical stability and non-toxicity.

Fauzi et al. [17] combine various fatty acids to create two kinds of eutectic mixtures to be cycle tested experimentally for their thermal reliability. The mixtures are myristic acid/palmitic acid/sodium myristate (MA/PA/SM) and myristic acid/palmitic acid/sodium palmitate (MA/PA/SP), and the authors claim these show good performance applicable for TES in domestic usage such as domestic water heating.

Kant et al. [18] studied the performance of five different fatty acids (capric acid, lauric acid, myristic acid, palmitic acid and stearic acid) in aluminium containers for a 2D numerical simulation based on finite element analysis in COMSOL Multiphysics. Their results show reports in terms of melting fraction, temperature variation and transition of solid-liquid interface. They conclude that the

maximum energy is stored by stearic acid and the minimum for capric acid under the same boundary conditions.

Nazir et al. [19] prepare a total of ten mixtures of fatty acid based eutectics for solid-liquid low to moderate temperature latent heat TES. They combine Palmitic acid, myristic acid, stearic acid, lauric acid and commercial PureTemp68 to create materials with lower operating temperature and higher latent heat. Results reveal the melting points range from 27 to 75°C approximately, with the latent heat ranging from 127 to 210kJ/kg, making them suitable for solar water heating, thermal management in buildings, space heating applications etc.

In regards to paraffin, Pagkalos et al. [20] compare and evaluate the use of PCM A44 (a paraffin) and water as thermal energy storage materials using a numerical approach. The domain created is a 2D axisymmetric computational one, simulated in ANSYS. The parameters investigated were the energy stored inside the material, the temperature of the HTF and the temperature of the storage medium. Results show the PCM A44 stores approximately 4 times more energy than water, yet water charges the system roughly 3 to 3.9 times (depending on the tube length) faster than the paraffin.

He et al. [21] investigate the performance of a water TES tank with encapsulated paraffin wax in a packed bed design compared to a conventional water TES tank. They have an experimental setup which consists of a cylindrical tank with a conical bottom which is 1.1m in height and has a 0.9m diameter. Results indicate larger energy storage density with the added PCMs, but longer charging time. Furthermore, when operating at the same flow rate, the stratification was also worse for the PCM tank, yet the influence of flow rate on a PCM filled tank was greater, which can be useful in applications with small flow rate.

Kousksou et al. [9] present an analysis of six paraffin types, with air as a working fluid, for a cylindrical tank. They conclude that the efficiency of the system increases with increasing the inlet velocity and decreasing the melting temperature of the PCMs.

Aldoss et al. [22] also provide a study involving the combination of three paraffin types with increasing melting temperatures in a packed bed. These paraffins are waxes denoted as PCM40, PCM50 and PCM60 based on their phase change temperatures. They propose the use of multi stage PCM designs to increase the performance of the system and conclude that, whilst adding a second stage to the TES significantly increases the melting temperature distribution in the charging process, three or more stages provide a less significant improvement. From a practical and economical point of view it is deemed inadvisable.

Focusing on the design of the system itself, these can fall under three main categories: single-tank, two-tank and heat exchangers. Commonly used heat exchangers include shell and tube ones [23, 24], where some are enhanced with fins [25]. Single and two-tank can contain fluid materials in them

or can be packed solid or encapsulated materials. A two tank system will use both tanks for separate hot and cold storage, whereas the single tank can use a thermocline to divide the hot and cold sections, or be used only for one (heating/cooling) and recharged as needed. The majority of research is done regarding cylindrical tanks [4, 21, 22, 26], but some have been known to use rectangular tanks too [27, 28]. Amongst other publications, there are a significant amount of studies regarding two-tank TES [29, 30], but some authors argue that using a single tank over a two-tank system can positively decrease and save up to 35% of the system's capital costs [31, 32].

For systems including tanks, an important parameter is the ratio between the length (L) or height (H) and diameter (D). Yang et al. [32] state cycle efficiency is improved with larger length ratios and higher tanks, adding that the tank height will directly influence temperature transition and output temperatures. They also add that a shorter tank will have a sharper temperature gradient and heat exchange zone compared to a taller tank. Angelini et al. [33] in their 14m height and 23.7m diameter tank design, found that stratification is improved in a high aspect ratio tank of height over diameter.

Klein et al. [34] consider various aspect ratios of 1, 2, 3, 4 and 5 (L/D) for their single tank packed bed. For each of these, four particle diameters (10, 16, 25 and 50mm) are also simulated. They conclude that for each analysed storage configuration the level of stored energy increased when increasing the aspect ratio and decreasing the particle diameter. Talukdar et al. [35] look into PCM for a finned heat exchanger TES in an energy backup system. They investigate several thicknesses (4.5cm, 5.0cm, 5.5cm, 6.0cm, 6.5cm and 7.0cm) for the PCM pack and model 3D computational fluid dynamics (CFD) simulation for both charging and discharging. They find that a pack of 6.5cm thickness with a higher number of fins solidifies faster, and has higher energy storage capacity and heat flux during melting.

Zanganeh et al. [36] assess the effect of operational and design parameters, such as diameter to height ratio, cone angle and particle diameter, on the performance of a thermocline TES based on a packed bed. The tested angles are 0, 10, 20 and 30° (all for a tank height of 25m), the different selected diameters are 10, 25 and 40mm (again for a 35m height tank) and the aspect ratios include 0.5, 0.75, 1, 1.25, 1.5, 1.75 and 2. The tank height for the different ratios varies from approximately 20 to 50m, whereas the diameters range from 25 to 40m roughly. They conclude that increasing the tank cone angle lowered the final discharge outflow temperature but raised the thermocline, allowing a smaller height. Decreasing the rock diameter resulted in a strong increase in pumping losses but a decrease in the drop of the final outflow temperature. Increasing the D/H ratio decreases the pumping losses but caused the final discharge outflow temperature to drop and thermal losses to increase.

This investigation focuses on the effect of the inlets on the heat distribution across the length of the tank for three different positions. The choice for a single cylindrical tank was due to it decreasing

the cost of the system compared to other designs. Paraffin was chosen as the storage medium due to its vast flexibility in terms of melting temperatures and the cost advantage over the fatty acids. A square tank with an aspect ratio of 1 was investigated, as there is a limited amount of research done on such systems. The PCM size of 25mm diameter was based on the article by Dong et al. [37] where the macroencapsulation for octadecane paraffin was carried out in a hollow steel ball of 22mm outer diameter.

2. Methodology

In this study we explored the possibility of a solid-liquid setup, with paraffin as the material, for a latent heat thermal energy storage system. Water was chosen as the heat transfer fluid (HTF) due to its suitable thermodynamic properties and the system operating temperature range. A packed bed design containing PCMs in encapsulated spheres was simulated, and the heating dynamics and influence of the various thermal and design parameters were evaluated.

2.1 System Parameters

The system consists of a 2D symmetrical single cylindrical tank domain, of 0.5m in height and diameter, packed with a set of 19x17 encapsulated spheres containing the selected PCM. The tank frame is 0.025m thick and the capsule is considered thin and negligible, with the sphere radius of 0.0125m. The HTF enters the system at a constant temperature of 90°C. The inlet velocities studied were 0.1m/s, 0.05m/s and 0.01m/s. The system initially starts with still water inside the tank at an ambient temperature of 20°C.

The main area of interest is the heating dynamics of the system and how it is affected by tank design, HTF velocity and PCM material properties. Two different designs were analysed, shown in Figure 1, where the PCMs are denoted as the blue square, the inlet is the top light blue line and the outlet is the bottom green line. Design A consists of a single inlet and outlet, both 0.12m in length. Design B consists of two inlets and a single outlet, all with dimensions 0.12m.

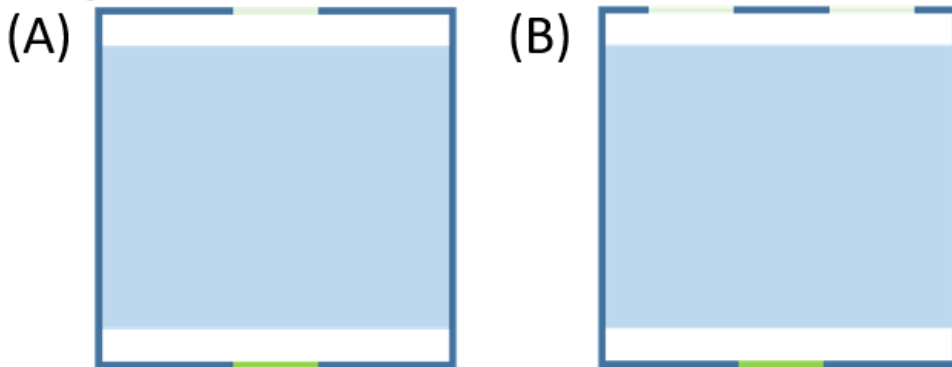


Figure 1: The two design types which are analysed in this paper

The temperatures were monitored at three selected positions: at the centre sphere, the top left sphere and the bottom left sphere, and the overall thermal gradient was recorded across the tank.

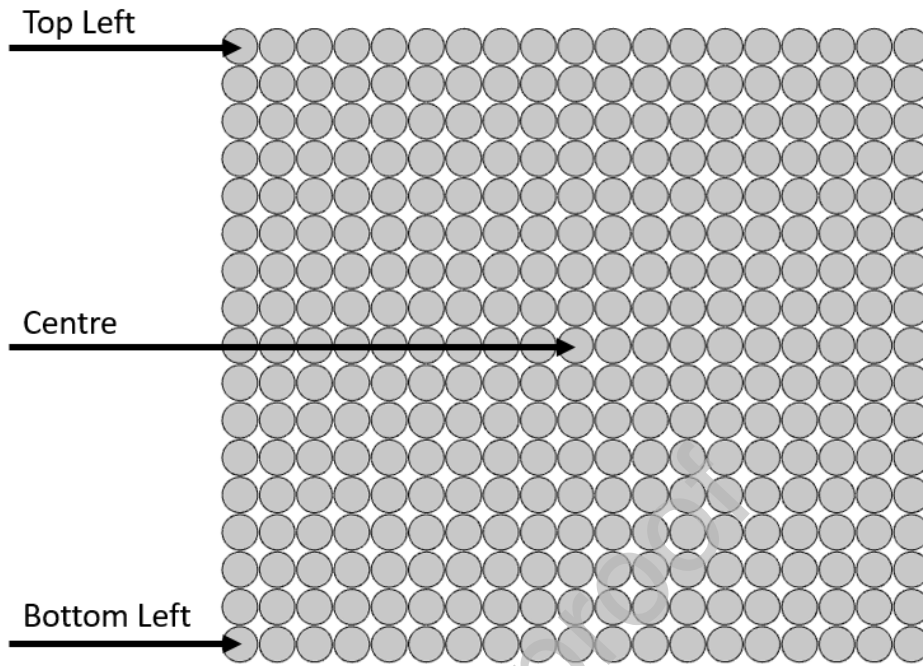


Figure 2: Three positions across the tank where the temperature will be recorded

The system mesh is generated by the software and was set to be extremely coarse and physics controlled, with approximately 138,000 mesh elements (mostly triangular prisms).

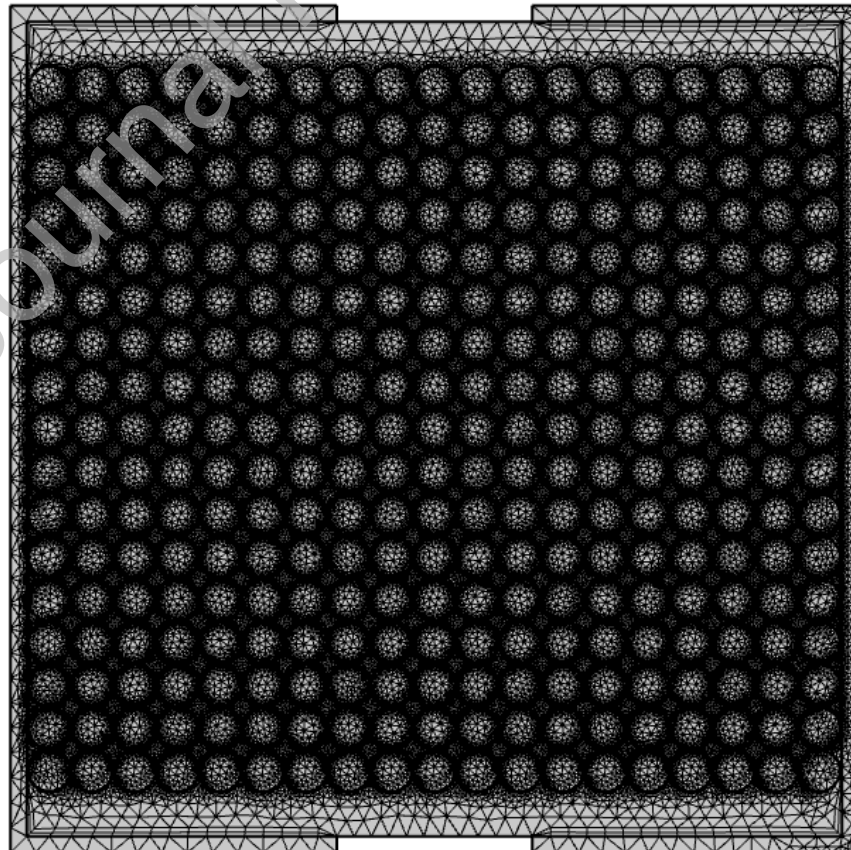


Figure 3: Physics generated 2D system mesh (COMSOL Multiphysics)

2.2 Boundary conditions and assumptions

The 2D simulation is run in COMSOL Multiphysics for 30 simulation minutes at 1 minute intervals. The model uses the “Laminar Flow” and “Heat Transfer in Fluids” physics, alongside the “Nonisothermal Flow” multi-physics. The mesh was approximately 140,000 mesh elements, mostly triangular prisms. The heat transfer problem was solved using the heat equation for non-uniform isotropic mediums and Fourier’s law:

$$\rho C_p \frac{\partial T}{\partial t} + \rho C_p u \cdot \nabla T + \nabla \cdot q = Q + Q_p + Q_{vd} \quad (3)$$

$$q = -k \nabla T \quad (4)$$

Where ρ is density, C_p is the heat capacity at constant pressure, T is temperature, t is time, u is velocity, q is the heat flux, Q is the heat source, Q_p is heat pressure work, Q_{vd} is heat viscous dissipation and k is the thermal conductivity.

The boundary conditions in the wall are no slip and the tangential velocity is equal to zero. The inlet is a fully developed velocity profile, whilst the outlet boundary condition is set to pressure, where initial pressure is zero and the model suppresses backflow. The HTF is modelled as laminar and incompressible, and materials are assumed to be homogeneous and isotropic. There are no heat transfers or losses due to radiation and the outside of the tank is perfectly insulated. Lastly, the spheres are modelled as circles that do not undergo deformation.

The tested PCM was Paraffin Wax. The relevant properties are presented in Table 1:

Table 1: Selected PCM for the study and its relevant properties [38]

Phase Changing Material (PCM)	Melting point (T_m) °C	Latent Heat of Fusion (L) kJ/kg	Density Solid / Liquid (ρ_s/ρ_l) kg/m ³	Thermal Conductivity Solid / Liquid (k_s/k_l) W/mK	Specific Heat Capacity Solid / Liquid (c_{ps}/c_{pl}) J/kgK
Paraffin Wax	55.55	190.0	825/755	0.230/0.200	2200/2100

2.3 Model validation

This model was validated using data from the publication by Elouali et al. [39]. The figure below shows the plot for a single phase model packed bed solid storage design, which uses pebbles as the storage medium. The COMSOL modelled system shows results that are in good agreement with Elouali et al. with the average deviation in temperatures being 5%.

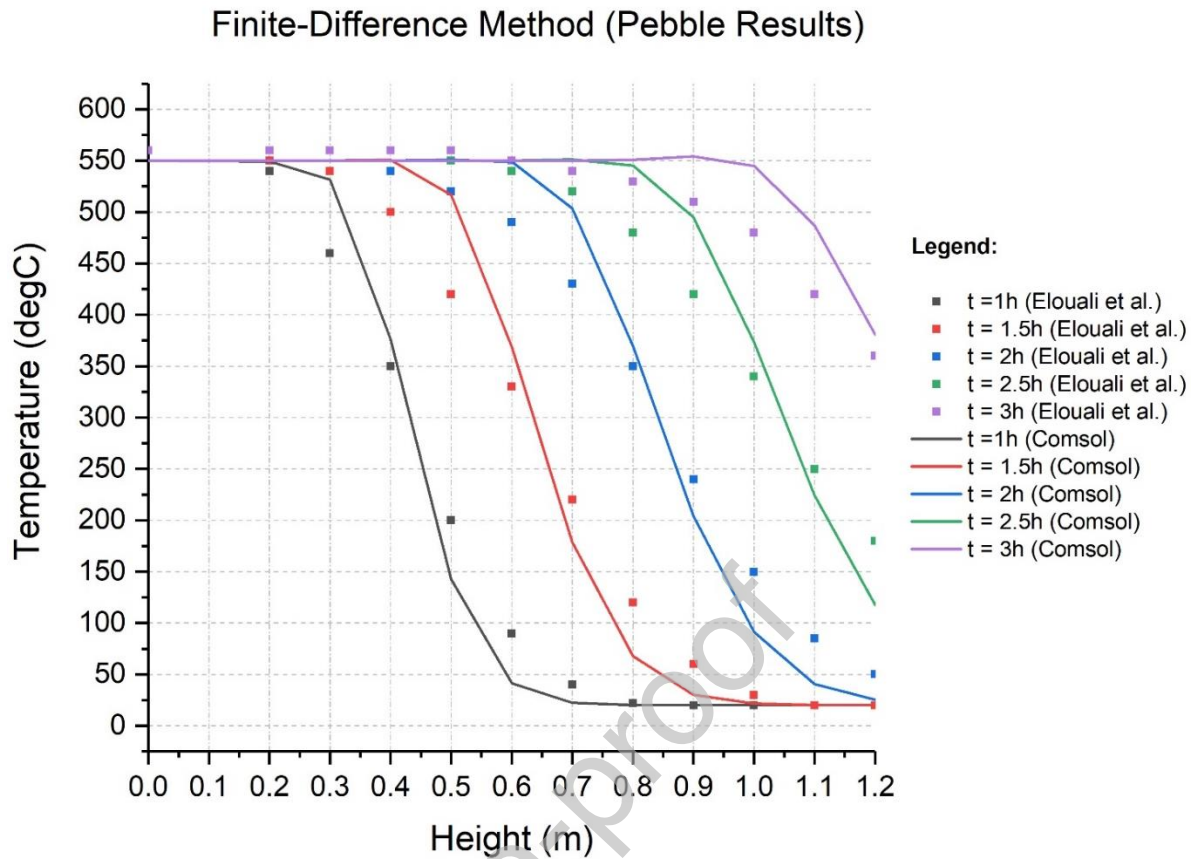


Figure 4: Model validation carried out based on the work carried out by Elouali et al.[39]

3. Results and Discussion

3.1 System Design

As the HTF enters the tank, the spheres closest to the inlet will naturally heat up the fastest. Hence, the fastest charging positions are the top ones, for both designs (seen in Figure 5). Nonetheless, all spheres will all commence heating up and absorbing heat as sensible heat, as shown by the constant increase in temperature seen in the lines between 0 and 7 minutes (approximately). After this, the phase change of the paraffin happens, where it absorbs the latent heat as denoted from the horizontal line from 7 to 17 minutes (approximately). Finally, the system again further absorbs sensible heat and curves as it reaches the HTF temperature of 90°C. This happens for all positions and for both designs, meaning the heating dynamics are not affected by these parameters.

The difference in temperature between the top, centre and bottom spheres after 30 minutes is almost negligible. Again, this is the same for both designs, A and B, where the charging time is essentially the same and the difference in temperatures has a maximum difference 5°C with a minimum of 1°C. Also, Design B reaches higher final temperatures than Design A, except these temperatures are in very close proximity to each other, which make the difference almost irrelevant.

This therefore concludes that the extra inlet is not advisable, as the single inlet is simpler and more cost effective design.

Figure 5 below shows both designs, for a set velocity of 0.1m/s, for all positions. Furthermore, the velocity profiles were different between one design and the other as can be seen in Figures 6 and 7, where it is seen that the addition of the second inlet allows for faster flow and increased velocity on the system and between the encapsulated PCM.

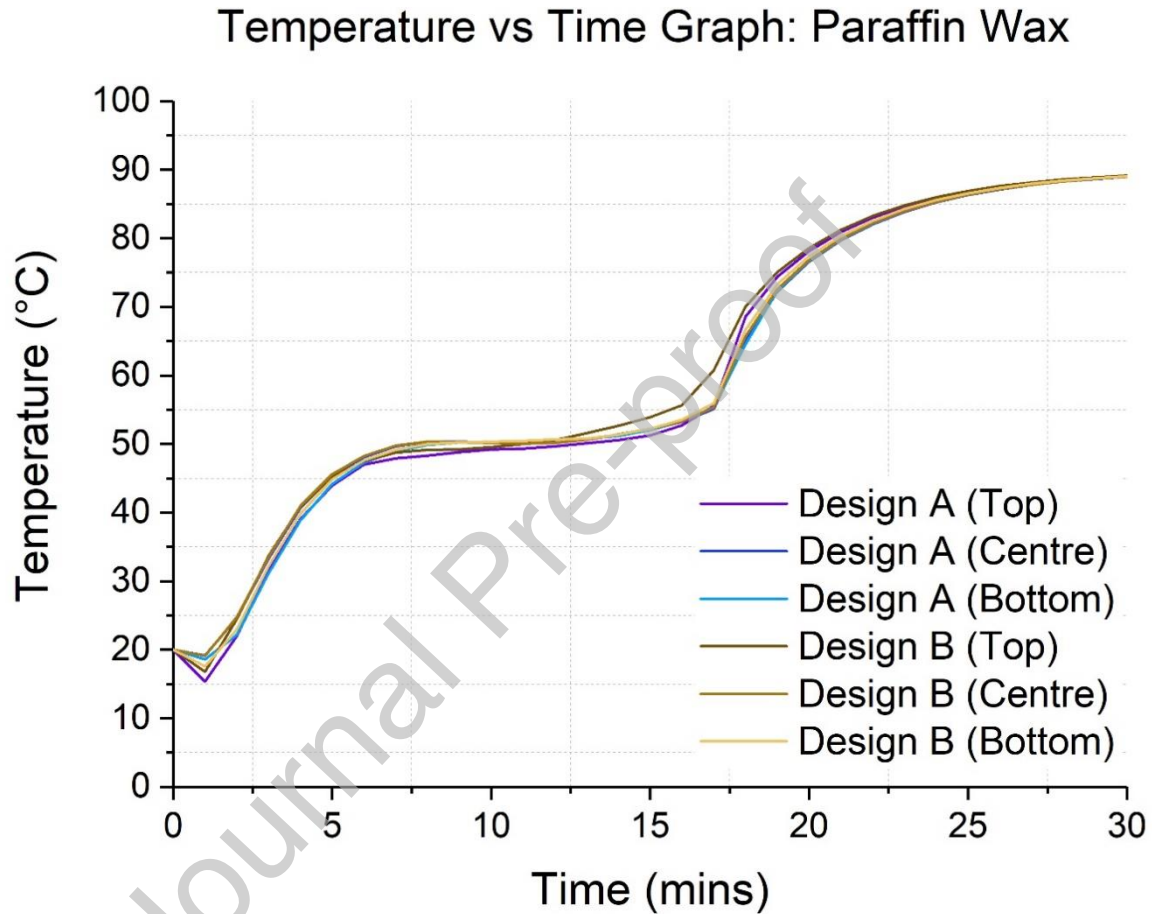


Figure 5: Temperature vs time graphs for both designs at a velocity of 0.1m/s

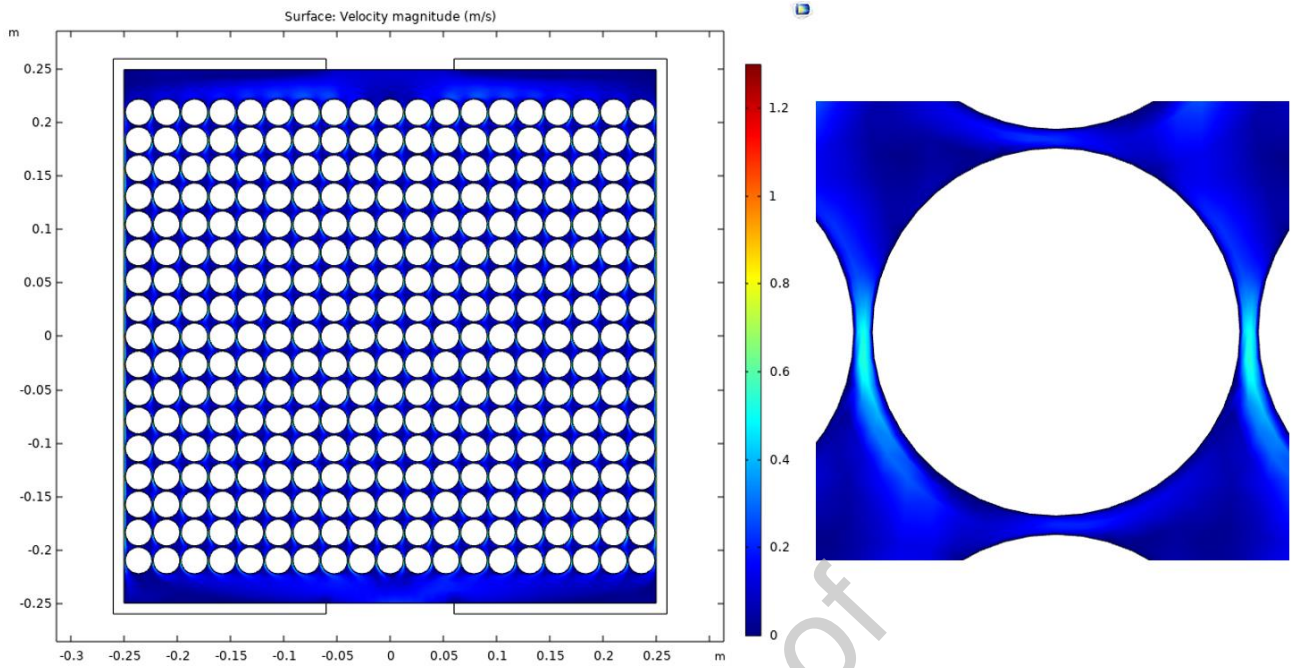


Figure 6: Velocity profile for design A for an inlet velocity of 0.1m/s and zoom-in of centre sphere

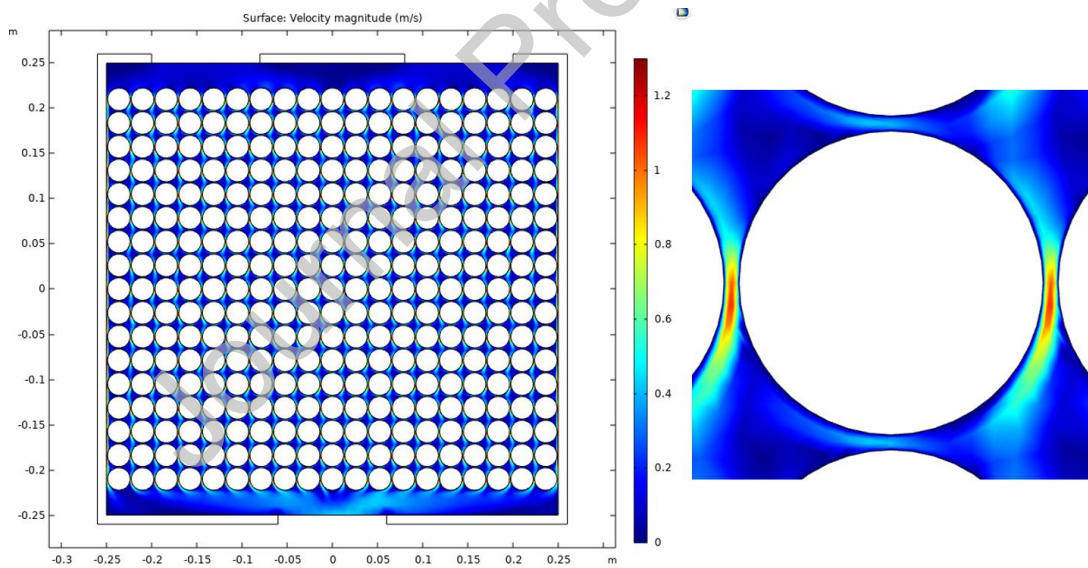


Figure 7: Velocity profile for design B for an inlet velocity of 0.1m/s and zoom-in of centre sphere

3.2 Effect of inlet velocity

Higher inlet velocity results in faster charging of the system and steeper heating dynamics (Figures 8 and 9). The lag is more significant in the bottom sphere than the top sphere, where the top sphere lines are almost superimposed at the end of the 30 minutes. From 0.1m/s to 0.05m/s the delay is not important, but when decreased further to 0.01m/s, it really compromises the charging of the bottom

sphere. There is an approximately 2 minute lag in the system before latent heat, and a final lag of roughly 5 minutes after latent heat. For the top sphere, the lag only accounts for a minute before and after phase change, but exists nonetheless. After the 30 minutes, the sphere that was the closest to reaching the HTF temperature was the top sphere at velocity 0.01m/s for Design B, with a percentage of 99.72%. The one that was furthest from the goal was the bottom sphere at velocity 0.01m/s for Design A with a percentage of 95.63%.

Changing the inlet velocity from maximum to minimum across the tested range in Design A led to a final temperature decrease of $\sim 0.3^{\circ}\text{C}$ for the top sphere, just under $\sim 1^{\circ}\text{C}$ for the centre sphere, and $\sim 3^{\circ}\text{C}$ for the bottom sphere (Table 2 in Appendices). For Design B, this difference was larger at $\sim 0.7^{\circ}\text{C}$ for the top sphere, $\sim 1.3^{\circ}\text{C}$ for the centre sphere and $\sim 1.1^{\circ}\text{C}$ for the bottom sphere. The largest difference happens for the centre sphere for Design B and for the bottom sphere for Design A. Furthermore, the differences are closer in terms of percentage in Design B but are more extreme for Design A. These differences, however, are minimal and can be classified as negligible for both designs.

In terms of heat absorption, lower inlet velocities compromise the total heat absorption for Design A, but again work best for Design B. The same pattern mentioned above about the final temperatures is repeated for the total heat absorption; the maximum heat absorption was again the top sphere at velocity 0.01m/s for Design B with a percentage of 99.85% (2225.52J), whereas the minimum was the bottom sphere at velocity 0.01m/s for Design A with a percentage of 97.58% (2174.91J). The total difference in heat absorbed between the highest and lowest was 50.61J, a value that again can be considered negligible.

The data suggests that the change in velocity could benefit or hinder the system based on the design and that there is no pattern linked to lower/higher velocities equalling a better performing system. Furthermore, the addition of a second inlet provides a higher heat transfer rate throughout the tank which causes less extreme temperature differences between the top and bottom spheres. This is probably due to the HTF entering and spreading across the tank in a more distributed manner.

Temperature vs Time Graph: Paraffin Wax (Bottom Sphere)

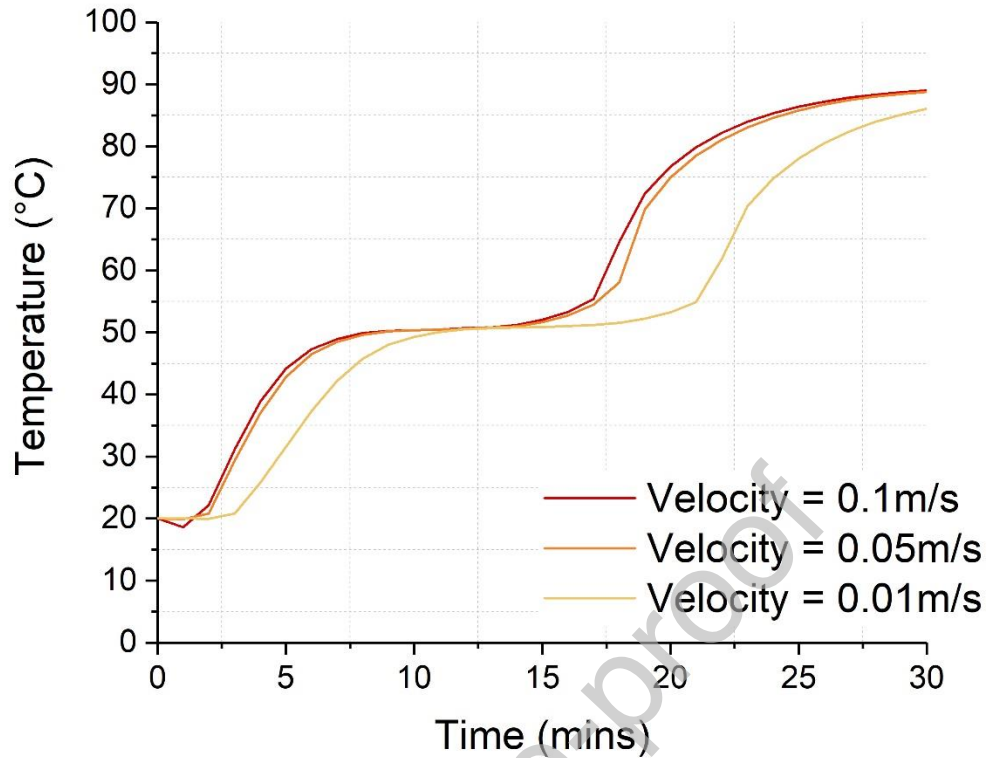


Figure 8: Temperature vs time graphs for all velocities, for Design A, for the bottom sphere

Temperature vs Time Graph: Paraffin Wax (Top Sphere)

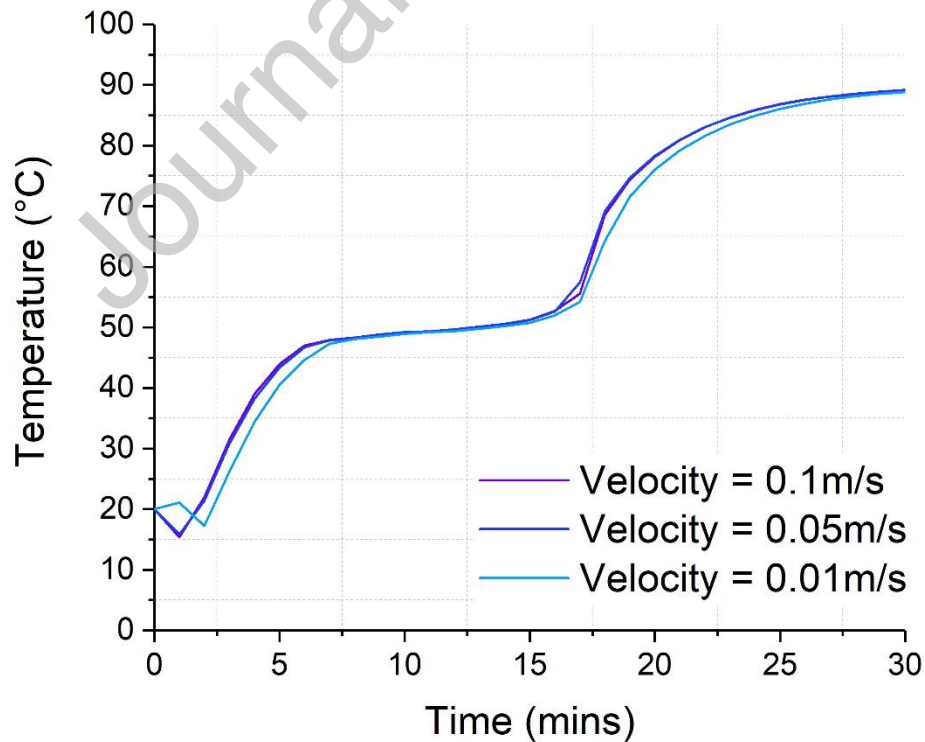


Figure 9: Temperature vs time graphs for all velocities, for Design A, for the top sphere

Conclusion

From the presented study, the following conclusions can be derived:

- Although an addition of a second inlet to the system yields higher final temperatures and improves the distribution of the HTF, allowing a better heat transfer rate, this change was marginal. Therefore, it is considered unfavourable.
- There is no one rule in regards to velocity, as a higher velocity or lower velocity at the inlet improves the heat transfer rate and allows higher temperatures and higher heat absorption depending on the design.
- Paraffin has proven to be a suitable material with favourable properties as a TES system, with benefits such as fast charging and good latent heat absorption.

References

- [1] H. E. Murdock, D. Gibb, T. André – REN21. Renewables 2019 Global Status Report (2019). Paris: REN21 Secretariat. ISBN 978-3-9818911-7-1
- [2] G. Alva, Y. Lin, G. Fang. **An overview of thermal energy storage systems**. Energy 144: 341-378 (2018). doi:10.1016/j.energy.2017.12.037
- [3] G. Alva, L. Liu, X. Huang, G. Fang. **Thermal energy storage materials and systems for solar energy applications**. Renewable and Sustainable Energy Reviews 68: 693-706 (2017). doi: 10.1016/j.rser.2016.10.021
- [4] R. Lugolole, A. Mawire, K.A. Lentswe, D. Okello, K. Nyeinga. **Thermal performance comparison of three sensible heat thermal energy storage systems during charging cycles**. Sustainable Energy Technologies and Assessments 30: 37-51 (2018). doi: 10.1016/j.seta.2018.09.002
- [5] A. Mehari, Z.Y. Xu, R.Z. Wang. **Thermally-pressurized sorption heat storage cycle with low charging temperature**. Energy 189: 116304 (2019). doi: 10.1016/j.energy.2019.116304
- [6] A. Maldonado-Alameda, A.M. Lacasta, J. Giro-Paloma, J.M. Chimenos, L. Haurie, J. Formosa. **Magnesium phosphate cements formulated with low grade magnesium oxide incorporating phase change materials for thermal energy storage**. Construction and Building Materials 155: 209-216 (2017). doi: 10.1016/j.conbuildmat.2017.07.227
- [7] C. N. Elias, V. N. Stathopoulos. **A comprehensive review of recent advances in materials aspects of phase change materials in thermal energy storage**. Energy Procedia 161: 385-394 (2019). doi: 10.1016/j.egypro.2019.02.101
- [8] E. Gonzalez-Roubaud, D. Perez-Osorio, C. Prieto. **Review of commercial thermal energy storage in concentrated solar power plants: Steam vs. molten salts**. Renewable and Sustainable Energy Reviews 80: 133-148 (2017). doi: 10.1016/j.rser.2017.05.084

- [9] T. Kousksou, F. Strub, J. Castaing Lasvignottes. **Second law analysis of latent thermal energy storage for solar system**. Solar Energy Materials & Solar Cells 91: 1275-1281 (2007). doi:10.1016/j.solmat.2007.04.029
- [10] T. Kousksou, P. Bruel, A. Jamil, T. ElRhafiki, Y. Zeraouli. **Energy storage: Applications and challenges**. Solar Energy Materials & Solar Cells 120: 59-80 (2013). doi: 10.1016/j.solmat.2013.08.015
- [11] A. Fallahi, G. Guldentrops, M. Tao, S. Granados-Focil, S. Van Dessel. **Review on solid-solid phase change materials for thermal energy storage: Molecular structure and thermal properties**. Applied Thermal Engineering 127: 1427-1441 (2017). doi: 10.1016/j.applthermaleng.2017.08.161
- [12] A. Sharma, V.V. Tyagi, C.R. Chen, B. Buddhi. **Review on thermal energy storage with phase change materials and applications**. Renewable and Sustainable Energy Reviews 13: 318-345 (2007). doi: 10.1016/j.rser.2007.10.005
- [13] P. Bose, V. A. Amirtham. **A review on thermal conductivity enhancement of paraffinwax as latent heat energy storage material**. Renewable and Sustainable Energy Reviews 65: 81-100 (2016). doi: 10.1016/j.rser.2016.06.071
- [14] D. Feldman, M.M. Shapiro, D. Banu, C.J. Fuks. **Fatty acids and their mixtures as phase-change materials for thermal energy storage**. Solar Energy Materials 18: 201-216 (1989). doi: 10.1016/0165-1633(89)90054-3
- [15] C. Amaral, R. Vicente, P.A.A.P. Marques, A. Barros-Timmons. **Phase change materials and carbon nanostructures for thermal energy storage: A literature review**. Renewable and Sustainable Energy Reviews 79: 1212-1228 (2017). doi: 10.1016/j.rser.2017.05.093
- [16] A. Sharma, L. D. Won, D. Buddhi, J. U. Park. **Numerical heat transfer studies of the fatty acids for different heat exchanger materials on the performance of a latent heat storage system**. Renewable Energy 30: 2179-2187 (2005). doi:10.1016/j.renene.2005.01.014
- [17] H. Fauzi, H.S.C Metselaar, T.M.I Mahlia, M. Silakhori, H. Chyuan Ong. **Thermal characteristics reliability of fatty acid binary mixtures as phase change materials (PCMs) for thermal energy storage applications**. Applied Thermal Engineering 80: 127-131 (2015). doi: 10.1016/j.applthermaleng.2015.01.047
- [18] K. Kant, A. Shukla, A. Sharma. **Performance evaluation of fatty acids as phase change material for thermal energy storage**. Journal of Energy Storage 6: 153-162 (2016). doi: 10.1016/j.est.2016.04.002
- [19] H. Nazir, M. Batool, M. Ali, A. M. Kannan. **Fatty acids based eutectic phase change system for thermal energy storage applications**. Applied Thermal Engineering 142: 466-475 (2018). doi: 10.1016/j.applthermaleng.2018.07.025
- [20] C. Pagkalos, G. Dogkas, M. K. Koukou, J. Konstantaras, K. Lymperis, M. Gr. Vrachopoulos. **Evaluation of water and paraffin PCM as storage media for use in thermal energy storage**

- applications: A numerical approach.** International Journal of Thermofluids 000: 100006 (2019). doi: 10.1016/j.ijft.2019.100006
- [21] Z. He, X. Wang, X. Du, M. Amjad, L. Yang, C. Xu. **Experiments on comparative performance of water thermocline storage tank with and without encapsulated paraffin wax packed bed.** Applied Thermal Engineering 147: 188-197 (2019). doi: 10.1016/j.applthermaleng.2018.10.051
- [22] T. K. Aldoss, M. M. Rahman. **Comparison between the single-PCM and multi-PCM thermal energy storage design.** Energy Conversion and Management 83: 79-87 (2014). doi: 10.1016/j.enconman.2014.03.047
- [23] L. A. Tse, G. B. Ganapathi, R. E. Wirz, A. S. Lavine. **Spatial and temporal modeling of sub and supercritical thermal energy storage.** Solar Energy 103: 402-410 (2014). doi: 10.1016/j.solener.2014.02.040
- [24] L. A. Tse, A. S. Lavine, R. B. Lakeh, R. E. Wirz. **Exergetic optimization and performance evaluation of multi-phase thermal energy storage systems.** Solar Energy 122: 396-408 (2015). doi: 10.1016/j.solener.2015.08.026
- [25] F. Agyenim, P. Eames, M. Smyth. **Experimental study on the melting and solidification behaviour of a medium temperature phase change storage material (Erythritol) system augmented with fins to power a LiBr/H₂O absorption cooling system.** Renewable Energy 36: 108-117 (2011). doi: 10.1016/j.renene.2010.06.005
- [26] M.A. Izquierdo-Barrientos, C. Sobrino, J.A. Almendros-Ibáñez. **Thermal energy storage in a fluidized bed of PCM.** Chemical Engineering Journal 230: 573-583 (2013). doi: 10.1016/j.cej.2013.06.112
- [27] A. Koca, H. F. Oztop, T. Koyun, Y. Varol. **Energy and exergy analysis of a latent heat storage system with phase change material for a solar collector.** Renewable Energy 33: 567-574 (2007). doi: 10.1016/j.renene.2007.03.012
- [28] F. Aghbalou, F. Badia, J. Illa. **Exergetic optimization of solar collector and thermal energy storage system.** International Journal of Heat and Mass Transfer 49: 1255-1263 (2005). doi: 10.1016/j.ijheatmasstransfer.2005.10.014
- [29] A. White, G. Parks, C. N. Markides. **Thermodynamic analysis of pumped thermal electricity storage.** Applied Thermal Engineering 53: 291-298 (2013). doi: 10.1016/j.applthermaleng.2012.03.030
- [30] J. D. McTigue, A. J. White, C. N. Markides. **Parametric studies and optimisation of pumped thermal electricity storage.** Applied Energy 137: 800-811 (2015). doi: 10.1016/j.apenergy.2014.08.039
- [31] M. Wu, C. Xu, Y. L. He. **Dynamic thermal performance analysis of a molten-salt packed-bed thermal energy storage system using PCM capsules.** Applied Energy 121: 184-195 (2014). doi: 10.1016/j.apenergy.2014.01.085

- [32] Z. Yang, S. V. Garimella. **Cyclic operation of molten-salt thermal energy storage in thermoclines for solar power plants**. Applied Energy 103: 256-265 (2012). doi: 10.1016/j.apenergy.2012.09.043
- [33] G. Angelini, A. Lucchini, G. Manzolini. **Comparison of thermocline molten salt storage performances to commercial two-tank configuration**. Energy Procedia 49: 694-704 (2014). doi: 10.1016/j.egypro.2014.03.075
- [34] P. Klein, T.H. Roos, T.J. Sheer. **Parametric analysis of a high temperature packed bed thermal storage design for a solar gas turbine**. Solar Energy 118: 59-73 (2015). doi: 10.1016/j.solener.2015.05.008
- [35] S. Talukdar, H. M. M. Afroz, M. A. Hossain, M.A. Aziz. **Heat transfer enhancement of charging and discharging of phase change materials and size optimisation of a latent thermal energy storage system for solar cold storage application**. Journal of Energy Storage 24: 100797 (2019). doi: 10.1016/j.est.2019.100797
- [36] G. Zanganeh, A. Pedretti, A. Haselbacher, A. Steinfeld. **Design of packed bed thermal energy storage systems for high-temperature industrial process heat**. Applied Energy 137: 812-822 (2015). doi: 10.1016/j.apenergy.2014.07.110
- [37] Z. Dong, H. Cui, W. Tang, D. Chen, H. Wen. **Development of Hollow Steel Ball Macro-Encapsulated PCM for Thermal Energy Storage Concrete**. Materials 9: 59 (2016). doi: 10.3390/ma9010059
- [38] B. Zalba, J. M. Marin, L. F. Cabeza, H. Mehling. **Review on thermal energy storage with phase change: materials, heat transfer analysis and applications**. Applied Thermal Engineering 23: 251-283 (2003). doi: 10.1016/S1359-4311(02)00192-8
- [39] A. Elouali, T. Kousksou, T. El Rhafiki, S. Hamdaoui, M. Mahdaoui, A. Allouhi, Y. Zeraoui. **Physical models for packed bed: Sensible heat storage systems**. Journal of Energy Storage 23: 69-78 (2019). doi: 10.1016/j.est.2019.03.004

Appendices

Table 2: Final temperature reached by spheres for all simulations

Velocity	Final temperature reached after 30minutes (°C)					
	Design (A)			Design (B)		
	Top	Centre	Bottom	Top	Centre	Bottom
0.1m/s	89.149	88.984	89.014	89.164	89.000	89.064
0.05m/s	89.117	88.857	88.807	88.869	88.616	88.675
0.01m/s	88.845	87.833	86.07	89.752	88.387	88.102

Table 3: Final temperature reached over maximum HTF temperature for all simulations

Velocity	Final temperature percentage difference (%)					
	Design (A)			Design (B)		
	Top	Centre	Bottom	Top	Centre	Bottom
0.1m/s	99.05%	98.87%	98.90%	99.07%	98.89%	98.96%
0.05m/s	99.02%	98.73%	98.67%	98.74%	98.46%	98.53%
0.01m/s	98.72%	97.59%	95.63%	99.72%	98.21%	97.89%

Table 4: Total final internal energy for all simulations (calculated with Equation 2)

Velocity	Total final internal energy (J)					
	Design (A)			Design (B)		
	Top	Centre	Bottom	Top	Centre	Bottom
0.1m/s	2217.23	2214.96	2215.38	2217.44	2215.18	2216.06
0.05m/s	2216.79	2213.22	2212.53	2213.38	2209.91	2210.72
0.01m/s	2213.05	2199.14	2174.91	2225.52	2206.76	2202.84

Table 5: Total final internal energy percentage difference between all simulations

Velocity	Total final internal percentage difference (%)					
	Design (A)			Design (B)		
	Top	Centre	Bottom	Top	Centre	Bottom
0.1m/s	99.48%	99.37%	99.39%	99.48%	99.38%	99.42%
0.05m/s	99.46%	99.30%	99.26%	99.30%	99.15%	99.18%
0.01m/s	99.29%	98.66%	97.58%	99.85%	99.01%	98.83%